Transformation, leaching and plant uptake simulations of 6:2 and 8:2 polyfluoroalkyl phosphate diesters (diPAPs) and related transformation products under near-natural conditions

Eva Weidemann[1*], René Lämmer[2], Bernd Göckener[2], Mark Bücking[2,3] and Matthias Gassmann[1]

Abstract

In response to the growing concern over PFAS contamination, employing models to simulate PFAS behavior in the environment becomes necessary. This facilitates evaluating risks tied to leaching into groundwater, adsorption in soil, plant uptake, entry into the food chain, and the conversion of precursors into persistent PFAS. We utilized the MACRO model to simulate the behavior of the precursors 6:2 diPAP and 8:2 diPAP using data from a 2-year lysimeter experiment, key compound parameters were optimized via the caRamel evolutionary algorithm. We assumed that the transformation of both diPAP precursors into stable PFAAs is influenced by temperature and soil moisture, similar to pesticide degradation by microorganisms. Results reveal that the model accurately represents transformation, leaching, soil retention, and plant uptake of diPAP and transformation products. A comparison with a lab-based soil column study supports the slower natural degradation of precursors, affirming our modeling approach. Temperature and soil moisture could indicate that a worst-case scenario for transformation product leaching into groundwater could occur during a mild summer with moderate evapotranspiration and heavy rainfall. Plant uptake involves multiple elements: PFAS availability in the root zone depends on prior degradation or presence. Increased moisture in the root zone favors PFAS uptake combined with temperatures high enough for prior biotransformation. The calculation of temperature and moisture-based conversion rates was adopted directly from MACRO. It is recommended to further investigate these effects to validate and possibly modify them.

Keywords PFAS, MACRO, Leaching simulation

*Correspondence:
Eva Weidemann
eva.weidemann@uni-kassel.de
Full list of author information is available at the end of the article

Weidemann *et al. Environmental Sciences Europe*   (2024) 36:63

Page 2 of 14

Background

Per- and polyfluoroalkyl substances (PFAS) are anthropogenic substances, which were created and used for products such as Teflon [1]. Currently, about 10,776 PFAS [2] are known, with a rapidly growing trend. While there are many useful fields of applications for PFAS, studies have already identified adverse effects associated with some PFAS, including persistence, bioaccumulation, and toxicity [3]. These effects vary within the group of PFAS, with most compounds not yet been investigated [4]. This includes, for example, perfluorooctanoic acid (PFOA), which is classified as a persistent compound within the subgroup of perfluoroalkyl acids (PFAA) [5]. PFAA are final transformation products of various biotransformable PFAS, referred as precursors [6]. These precursors include the group of polyfluoroalkyl phosphate diesters (diPAP). 6:2 and 8:2 diPAP [7], two important representatives of this group, are focused in the present study, simulating their biotransformation and leaching of transformation products in soil.

DiPAPs are used in the paper industry as grease and water repellent agents [8] and have already been detected in various environmental compartments such as soils [9], lakes [10] and indoor dust [11]. Once diPAPs are present in the soil, they are rather immobile due to their high sorption potential, but continue to release their transformation products [7]. PFAA, the mobile final transformation products of 6:2 diPAP and 8:2 diPAP [7], can rapidly enter the food web through plant uptake [12] or leach into groundwater [13], which may be a problem for several decades [14].

Due to the extensive range of PFAS and their diverse properties, there are currently gaps in our knowledge, particularly concerning the behavior of PFAS in the vadose zone. Studies involving non-degradable PFAS have shown that they exhibit lower recovery rates as the chain length increases [7, 15]. This phenomenon is often attributed to non-extractable residues (NER) [7], "irreversible sorption" [16] or "immobilized" compounds [15], all of which essentially have similar meanings. It has been established for other substances that they can form NER in soil through various mechanisms [17]. Although the process is not well understood, it has been frequently cited as a potential cause for a mass balance gap of PFAS in soil environments [7, 18, 19]. Several studies have also investigated the sorption of PFAS in soil. Fabregat-Palau et al. [20] attempted to estimate a sorption coefficient based on soil composition and chain length for a few PFAA but with significant uncertainties. Therefore, the estimate can only serve as an initial approximation due to the multitude of influencing factors. The study highlighted that the organic carbon content and the mineral soil fraction (clay and silt) have an impact on sorption, in addition to compound properties. However, the influence of these factors can vary depending on other parameters, such as the presence of other organic compounds or ions [21]. Understanding NER formation and sorption is crucial for estimating the potential of PFAS release from NER into soil.

The transformation pathways of certain precursors have been studied and documented [19, 22, 23]. However, transformation rates are often determined under constant environmental conditions [7, 19] and, in some cases, based on only two data points, assuming a uniform transformation rate [7, 12, 24]. It is important to note that transformation rates can be influenced by various factors. Firstly, the NER fraction may increase over time due to soil aging effects, as described in Cheng et al. [25] for organic pollutants. Consequently, the fraction of precursor available for transformation may decrease over time. Secondly, if microorganisms are involved in the transformation process, as observed in the transformation of diPAPs [19], parameters that influence microbial productivity also affect the transformation rate. These parameters include temperature [26, 27], oxygen availability [26, 27], soil water content [28, 29], the ability of plants to influence microbial communities [30], the strains of microorganism [31] and their environmental preferences, and the availability of nutrients [26, 27]. These diverse factors highlight the need to investigate their impact on precursor transformation to better predict the variability of transformation rates. Understanding these influencing factors can be used to model precursor transformation, enabling better estimations of substance behavior in contaminated soils.

Various models are available for simulating transformation and leaching processes in the vadose zone. These models were initially developed for pesticide registration purposes [32], but have been applied to other substances as well. Examples of such applications include veterinary antibiotics [33], pharmaceuticals [34] and nutrients [35]. Simulation studies involving different PFAS, primarily non-degradable ones [36], have also been conducted using various models such as HYDRUS [37] and MACRO [38]. These studies have examined environmental conditions such including saturated [39, 40] and unsaturated soils [18, 37, 38, 41], laboratory settings [41] and field conditions [18, 38]. Additionally, they have investigated various processes such as NER formation [38] and sorption at the air–water interface [37]. In existing models processes are limited to the leaching of PFAA [18, 37–39, 41–43], transformation of diPAP and leaching of PFAA [41], the transformation

of PAP [19], the uptake of PFAA in plants [44] and the behavior in the saturated zone [39, 42, 43, 45]. Additionally, a further overview is given in [36].

Available simulation studies focusing on precursor transformation in the vadose zone have primarily focused on areas contaminated with Aqueous Film-Forming Foam (AFFF) [46, 47]. However, a laboratory-based simulation study using unsaturated soil columns has been conducted to investigate the transformation of 6:2 and 8:2 diPAP [41]. The results of this study revealed that the biotransformation rate was not constant, indicating that changing conditions such as soil water content and oxygen availability influenced the transformation process.

In the present simulation study, we aimed to simulate the transformation of 6:2 diPAP and 8:2 diPAP, as well as related processes such as substance leaching, sorption and plant uptake, using data from a lysimeter study [24]. To the best of our knowledge, there is currently no existing simulation study that specifically addresses the transformation, leaching and plant uptake of transformation products of diPAPs and diPAPs in the vadose zone under near-natural conditions.

Materials and methods

Lysimeter study

In the 2-year lysimeter study in Schmallenberg, Germany [24], four lysimeters were set up to investigate the behavior of 6:2 and 8:2 diPAP individually in a duplicate setup each. The target concentration of diPAPs were 2 mg/kg dry matter for the upper soil half, having a total input mass of 628.5 mg in each lysimeter, which corresponds to a molar amount of 0.80 mmol (6:2 diPAP) and 0.63 mmol (8:2 diPAP). To prevent erosion, grass was planted on the surface of the lysimeters. The lysimeters were exposed to natural climate conditions and were not artificially watered.

Throughout the study, samples of percolate were collected at irregular intervals from the bottom of the lysimeters at 65 cm. The topsoil includes the soil until a depth of 25 cm, the subsoil the depth from 25 cm down to 60 cm and a gravel layer was added from a depth of 60 cm down to 65 cm. Grass samples were collected each year, and soil samples were obtained from five different depths at the end of study. Two methods were used to quantify PFAS, with detailed information provided in the original article [24]. The results presented in the study focus on the target method using tetrabutylammonium hydrogensulfate to quantify individual PFAS masses.

For the simulation study, values given in [24] are converted from concentrations to masses. All used values are listed in Additional file 1: Tables S3–8 in the

supporting information, as well as an overview of the mass balance is shown in Additional file 1: Fig. S1.

The MACRO model

MACRO is a 1D numerical model used for simulating solute transport and water flow in the vadose zone [48]. Originally developed for pesticide registration procedures, MACRO has been adapted for studying various substances [33, 38]. In this simulation study, MACRO version 5.2 is used in the command line version, and parameter changes are controlled using GNU R. The macroutils package (version 1.15.0), recommended by MACRO developers [49], is employed to convert simulation results.

The model incorporates several key features that are relevant to the present study. The actual evapotranspiration is calculated based on input data of temperature and potential evapotranspiration. The potential evapotranspiration is partitioned into potential transpiration and potential evaporation via calculation of a fraction intercepted by the transpiring canopy surfaces and by dead plant material as well as a fraction which reaches the soil surface, respectively [50]. Both fractions are calculated using values of (green) leaf area index [50]. The actual evaporation is calculated with the value of potential evapotranspiration and the actual transpiration is calculated by using a function of the water stress index accounting for the water content and the distribution of roots [48].

Water flow and substance transport are simulated using two dual-permeable domains: micropores and macropores. Solute transport is influenced by various substance parameters, including the sorption coefficient K_D, the linearity of sorption described by the Freundlich n parameter, anionic exclusion θ_{AE}, and transformation in all four domains (liquid/solid phase of micro-/macropores). Solute parameters can be adjusted individually for each soil horizon.

The actual transformation rate μ_D of the substances is calculated by

$$\mu_D = \mu_{\text{ref},D} \cdot F_w \cdot F_t, \tag{1}$$

using the reference transformation rate $\mu_{ref,D}$ and factors depending on temperature F_t and soil water content F_w. The factor F_t, which represents the influence of temperature on the transformation rate, is calculated using a three-section defined function:

$$F_t = e^{\alpha(T - T_{\text{ref}})} \text{ with } T > 5\,°\text{C}, \tag{2}$$

$$F_t = \left(\frac{T}{5}\right) e^{\alpha(5 - T_{ref})} \text{ with } 0 \leq T \leq 5\,°\text{C}, \tag{3}$$

$$F_t = 0 \text{ with } T < 0 \,^\circ\text{C}. \tag{4}$$

The function takes into account the reference temperature T_{ref} at which the transformation rate $\mu_{ref,D}$ was measured, the current temperature T and a parameter α. The default value of α is 0.08 (–) on the basis of Boesten, Linden [51]. Setting α to zero removes the temperature effect, while higher values of α amplify the impact of temperature on the transformation rate.

The factor F_w was updated from MACRO version 5.0 to 5.2 [52], using a different approach based on the work of Schroll et al. [53]. F_w is defined as a three-section function that depends on the current soil water content θ:

$$F_w = 0 \text{ with } \theta < 0.5\theta_w, \tag{5}$$

$$F_w = \left(\frac{\theta - 0.5\theta_w}{\theta_{100} - 0.5\theta_w} \right)^B \text{ with } 0.5\theta_w < \theta < \theta_{100}, \tag{6}$$

$$F_t = 1 \text{ with } \theta > \theta_{100}. \tag{7}$$

In very dry conditions, well below the soil water content at wilting point θ_w, the transformation rate is set to zero (5). As the soil water content increases until a water content corresponding to a pressure head of −100 cm is reached θ_{100}, F_w can have values between 0 and 1 (6). In very moist conditions (7), the conditions are considered ideal, and F_w is set to 1, which is the maximum value. The parameter B can be set to zero to eliminate the influence of F_w, provided that the soil water content does not fall within the range described by Eq. (5).

MACRO does not have explicit built-in support for modeling NER. However, a possible workaround has been used in previous simulations [33, 38], where NER were modeled by using the transformation rate in the solid phase of the micropores.

Plant uptake U_c is calculated by

$$U_c = f_c \cdot S_r \cdot c', \tag{8}$$

multiplying the solute concentration factor of the transpiration stream f_c, the root water uptake volume S_r and the solute concentration c'.

Model parameterization

In the MACRO model, a free flow situation at the bottom outlet and a variable water input by precipitation was chosen as boundary conditions. Precipitation and temperature data were obtained from a weather station situated at the lysimeter site. In cases of missing data, nearby weather stations were utilized as substitutes. Daily potential evapotranspiration was derived from raster data provided by the DWD (German Weather Service) [54]. Obtained raster data were calculated by DWD on the basis of the agrometeorological model AMBAV (Agricultural meteorological calculation of the current evaporation) for weather stations since 1991 and a multiple linear regression [55]. The grass was simulated as an annual crop using estimated parameter values (Additional file 1: Table S11). Physical soil data were measured (Additional file 1: Table S1). Soil parameters were calculated using the pedotransfer function FOOT-PRINT, which is part of the MACRO software. Initial soil water content and a selection of soil parameters were employed to calibrate the water flow (see Additional file 1: Table S9). Substance parameters used for optimizing the solute transport can be found in Table 1 and cover the K_D value, anion exclusion θ_{AE}, Freundlich n and the NER rate $\mu_{ref,s,mi}$. The parameters were varied for the two main transformation products of 6:2 diPAP perfluoropentanoic acid (PFPeA) and perfluorohexanoic acid (PFHxA) and the two main transformation products of 8:2 diPAP perfluoroheptanoic acid (PFHpA) and perfluorooctanoic acid (PFOA). All four transformation products belong to the group of the perfluorocarboxylic acids (PFCA), which belong to the PFAA group, and will be abbreviated with PFCA', if they

Table 1 Substance related parameter used for optimization. n.d. not determined

	Dimension	Precursors		PFCA'			
		6:2 diPAP	8:2 diPAP	PFPeA	PFHxA	PFHpA	PFOA
K_D	l/kg	1–100	1–100	0–0.40	0–0.72	0–1.25	0–3.50
θ_{AE}	%	–	–	0–10	0–10	0–5	0–5
Freundlich n	–	0.7–1.3	0.7–1.3	0.7–1.3	0.7–1.3	0.7–1.3	0.7–1.3
$\mu_{ref,s,mi}$	1/days	n.d	n.d	–	–	–	0–1
$\mu_{ref,l,mi}$	1/days	2	2	–	–	–	–
f_c	–	0–1	0–1	0–1	0–1	0–1	0–1

K_D = distribution coefficient, θ_{ae} = anion exclusion, $\mu_{ref,s,mi}$ = NER formation in the solid phase of the micropores, $\mu_{ref,l,mi}$ = transformation rate in the liquid phase of the micropores

6:2 diPAP: 6:2 polyfluoroalkyl phosphate diesters, 8:2 diPAP: 8:2 polyfluoroalkyl phosphate diesters, PFCA': perfluorocarboxylic acids transformation product of a precursor, PFPeA: perfluoropentanoic acid, PFHxA: perfluorohexanoic acid, PFHpA: perfluoroheptanoic acid, PFOA: perfluorooctanoic acid

emerged from a precursor. The K_D value was the only substance parameter which was varied for upper and lower soil separately, to reduce the amount of parameters within the optimization. The solute concentration factor f_c was calibrated using the entire interval from 0 up to 1 (see Table 1).

Initial diPAP masses in soil were set to recovered masses of the lysimeter study [24]: 401.9 mg and 522.7 mg for 6:2 diPAP and 8:2 diPAP, respectively, including their transformation products. The original mass input into the lysimeter for each compound was 628.5 mg. This approach was adopted due to uncertainties regarding the fate of the not recovered masses of precursors. NER were only simulated for PFOA, because of results given in [41]. The transformed masses were divided into multiple transformation products based on the formation fractions (*ff*) provided in Table 2. Formation fractions were determined using the amount of substance (mol), considering that two molecules of PFCA are equivalent to one molecule of diPAP [56]:

$$\text{ff} = \frac{m_{PFCA'}}{m_{diPAP'}}. \qquad (9)$$

It was observed that under sterile conditions, there was hardly any degradation of diPAPs [19], indicating the likely influence of temperature and moisture content, as they have a demonstrable impact on microorganisms [57]. So, the approach followed here considers the degradation rate being influenced by temperature and moisture content, which is also similar to pesticides [57]. For the gravel layer no sorption and no degradation was assumed.

Evaluation of model performance and modeling strategy
Goodness-of-fit values
The Kling–Gupta efficiency *KGE* [58] is calculated by

$$\text{KGE}_x = 1 - \sqrt{(r_x - 1)^2 + (\alpha - 1)^2 + (\beta - 1)^2}, \qquad (10)$$

Table 2 Formation fraction values used in the model

PFCA'	6:2 diPAP		8:2 diPAP	
	Mass	*ff*	Mass	*ff*
	mg	–	mg	–
PFBA	4.3	0.03	1.1	0.01
PFPeA	58.3	0.38	3.3	0.02
PFHxA	47.2	0.31	4.4	0.02
PFHpA	0.1	<0.01	16.6	0.08
PFOA	–	–	133.0	0.67

The formation fraction (*ff*) is calculated using the observed recovered transformed mass of 154.6 mg (6:2 diPAP') and 197.1 mg (8:2 diPAP')

$$\text{with } \alpha = \frac{s_x(\text{m})}{s_x(\text{o})}, \ \beta = \frac{\overline{m_x}}{\overline{o_x}}, \qquad (11)$$

using the Pearson correlation coefficient between simulated and observed values r_x, a quotient of standard deviations s_x, the average of simulated values $\overline{m_x}$ and the observed values $\overline{o_x}$.

The root mean square error *RMSE* is calculated by

$$\text{RMSE} = \left(\frac{1}{n} \sum_{t=1}^{n} (m_t - o_t)^2 \right)^{1/2}, \qquad (12)$$

using modeled values m_t and observed values o_t to create a mean absolute deviation of modeled values. For both objectives (*KGE, RMSE*), the hydroGOF (0.4–0) package was used.

Modeling strategy
The optimization was performed using the caRamel evolutionary algorithm [59] and 10,000 simulation runs. The transformation rate was influenced by both soil temperature and water content as described by Eq. (1). In each simulation run (Fig. 1), a parameter set was used, which included the soil parameters Van Genuchten's alpha (0.02–1 cm^{-1}), saturated hydraulic conductivity (50–150 mm h^{-1}), initial volumetric soil water content of subsoil and topsoil (20–25%), as well as substance parameters of diPAP and PFAA transformation products (see Table 1).

A modeling run was started using only soil parameters, soil water content and substance parameters of diPAPs. The results of this simulation as well as the substance parameters of the first transformation product were then used to simulate the leaching of the first transformation product, which was PFHpA in case of 8:2 diPAP. The same was done for the second transformation product PFOA. After a complete simulation, obtained values were compared to measured values via an objective function. The same was done for 6:2 diPAP and its transformation products. To evaluate the performance of each simulation run, four objectives were used. The *KGE* (9) was employed to evaluate the water flow and the *RMSE* was used to evaluate both transformation product masses observed in the percolate. Additionally, a simple difference between the observed and modeled values was minimized to assess the transformed diPAP mass. The optimization algorithm used the evaluation of these objective functions to create new parameter sets for subsequent simulation runs, aiming to improve the agreement between the model predictions and observed data.

After a complete optimization process, the simulations included in the Pareto front (best 500 and then
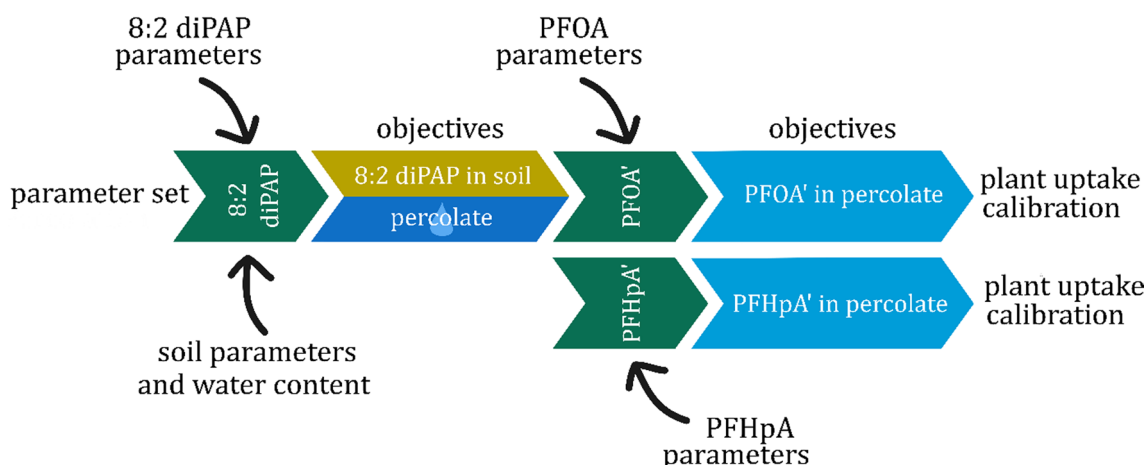
Fig. 1 Schematic of modeling strategy with 8:2 diPAP as example

90%-quartile of every of the four objectives) were selected for the calibration of the plant uptake of PFAA transformation products. This calibration process was separated from the optimization process and involved adjusting the solute concentration factor f_c. To calibrate f_c, the interval bisection method was used. This method involves iteratively adjusting the factor f_c within an interval and evaluating the goodness-of-fit with the observed data until the deviation from the observed values was less than or equal to 1%. The mean deviation of the substance uptake by plants for both years was used as a measure of the goodness-of-fit.

Results and discussion
Simulation results
The result of the optimizations were 314 simulations (6:2 diPAP) and 313 simulations (8:2 diPAP), that met the previously defined criteria. The water flow could be reproduced with good quality measures ($KGE_{6:2\ diPAP} = 0.78$–0.86, $KGE_{8:2\ diPAP} = 0.85$–0.86). This provided a solid foundation for simulating substance leaching. It is important to note that results obtained in controlled laboratory environments, such as the soil column study, may differ from natural conditions due to fewer variations in environmental factors like temperature and precipitation.

PFAS in percolate
In Fig. 2 the results of all chosen transformation product simulations in the period of April 2019 until April 2021 are shown. Until April 2020, all peaks and almost all observed values are covered by the simulations. Especially leaching dynamics of PFHpA and PFOA are well represented with only little deviations. Regarding PFPeA and PFHxA the dynamics are well represented as well,

but wide simulation ranges are notable, which could be related to variations in the modeled values of water fluxes (see Additional files 1: Fig. S2). The variations between modeled and observed percolate were also found for 8:2 diPAP lysimeters, but the influence of the variation may have been higher on the more mobile PFPeA and PFHxA. An overestimation of 6:2 diPAP transformation products masses (see Fig. 3) also influenced the leaching of both substances.

PFAS in soil
The modeling of the amount of diPAP, which is still adsorbed to soil particles, and its transformation products (PFPeA, PFHxA, PFHpA, PFOA), as shown in Fig. 3, was well-matched by the model, especially the dynamics with soil depth. Observed values of diPAPs in soil layers were all in the range of simulated values.

The best compromise overestimated the transformed amount of 6:2 diPAP. A high uncertainty of values can be found for the transformation products of 6:2 diPAP, PFPeA and PFHxA, although observed values are all within modeled ranges. The high uncertainty was only found in the upper two soil layers, whereby only outliers were recognized in the lower soil layers. This might be connected, to the simulations runs, in which transformed 6:2 diPAP mass was overestimated, or simulation runs, in which the highest K_D-values were used for a better representation of leaching from the bottom layer.

The transformed masses of 8:2 diPAP were underestimated in the simulation of the best compromise for the two upper soil layers. The amount in the third layer of 8:2 diPAP was highly underestimated, which could be the result of the third layer being the transition layer from initially contaminated soil to uncontaminated soil. Adsorption masses of PFHpA were underestimated
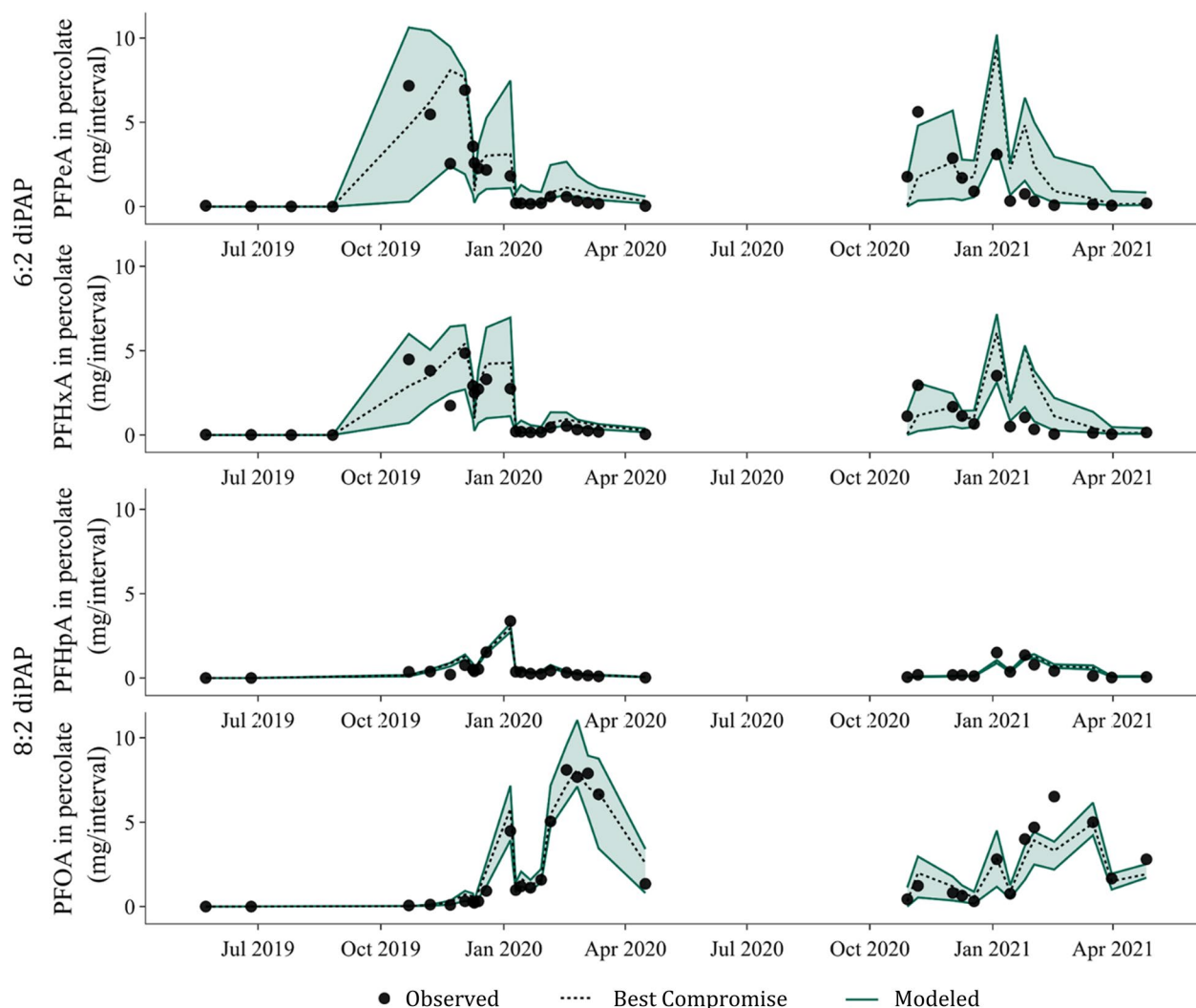
Fig. 2 Observed and modeled values of transformation products leaching of 6:2 diPAP (PFPeA, PFHxA) and 8:2 diPAP (PFHpA, PFOA) in mg/interval

in the upper two soil layers and overestimated in the lower soil layers. PFOA was also underestimated in every soil layer, but the increasing dynamic with soil depth was well simulated. Changing soil parameters may not have been expedient, because PFHpA masses were overestimated and PFOA masses underestimated. An improvement of one value would have worsened the fitting of other values, which is already covered by the pareto front of the optimization algorithm. A variation of the *ff* value might have improved the simulation results, which was not done due to the availability of the measured value. But the underestimation of simulated transformed 8:2 diPAP, would have been compensated by increasing the *ff* value of PFHpA and PFOA.

Plant uptake of PFAS

The decreasing uptake of PFPeA and PFHxA in the grass from 2019 to 2020 and the magnitudes were well represented by the model (Fig. 4): The best compromises have only slight deviations from the observed values and the distribution of values was broad, but still in the same order of magnitude. However, observed uptakes of PFHpA and PFOA were similar for both years, but were also represented by a decrease in the model, resulting in an underestimation of values in 2020 and an overestimation for PFHpA in 2019. One reason for the decreasing uptake in the model could be a decreasing availability of substance in the soil, since the amount of precursor also decreased over time. Further, the water content in the
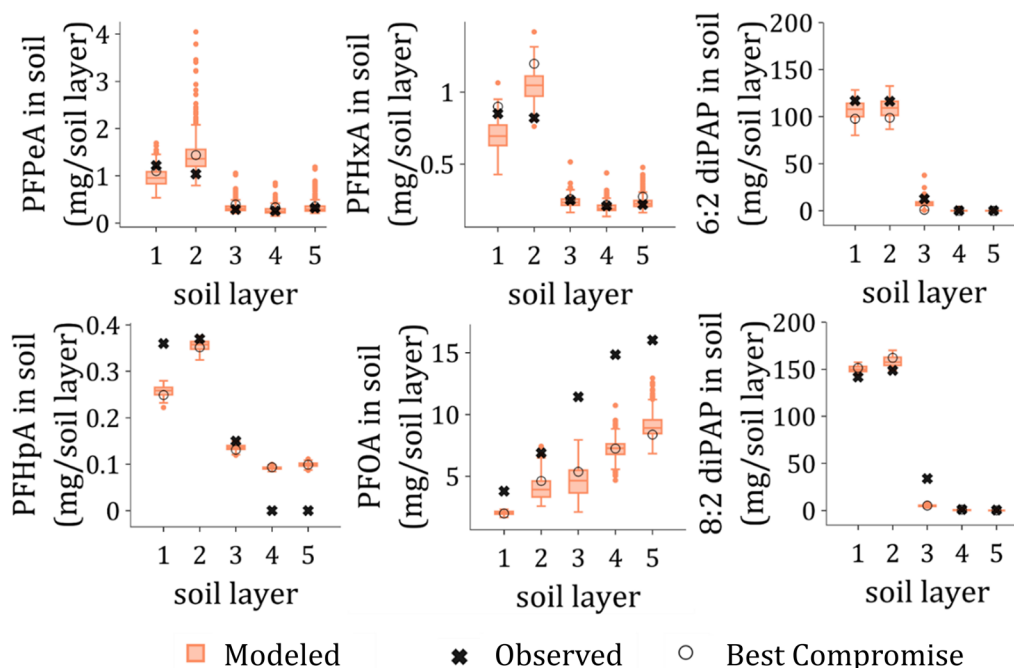
Fig. 3 Observed and modeled values of 6:2 diPAP and 8:2 diPAP and transformation products of 6:2 diPAP (PFPeA, PFHxA) and 8:2 diPAP (PFHpA, PFOA) in mg/soil layer. The order is from topsoil (1) to subsoil (5)
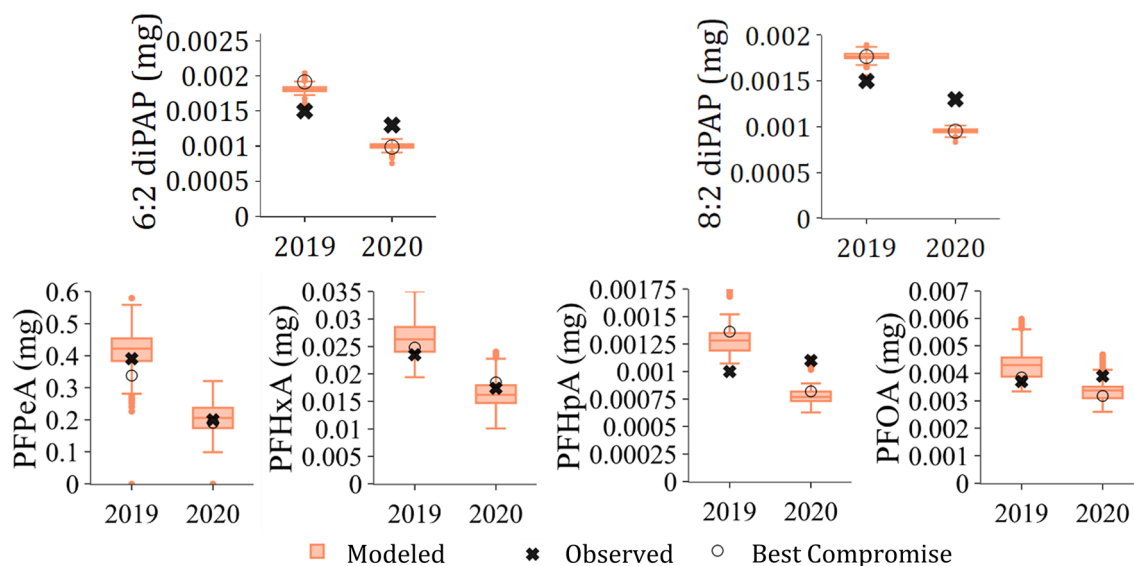

Fig. 4 Observed and modeled plant uptake of 6:2 diPAP and 8:2 diPAP and transformation products PFPeA, PFHxA (6:2 diPAP) and PFHpA, PFOA (8:2 diPAP) in mg/year

soil was lower in 2020 due to lower precipitation than in 2019. A comparison of the vegetation period April to August shows a difference of 122 L/m² (2019: 325 L/m², 2020: 204 L/m²). Looking into air temperature (26.04.–31.08), both years were similar, with 2020 being slightly colder (2019: $T_{mean} = 13.4$ °C, standard deviation = 5.7 °C;

2020: $T_{mean} = 13.0$ °C, standard deviation = 4.7 °C). A lower soil water content could have influenced the transformation rate as well as the availability of substances for the grass. The question arises why this dynamic cannot be found for PFHpA and PFOA. In 2019 an overestimation and in 2020 an underestimation of simulated values

can be found (Fig. 4). In case of simulated uptake values in 2019, an overestimation of transformed PFOA und PFHpA as well as their precursor 8:2 diPAP in the upper soil is likely the reason for an overestimated uptake. In case of 2020, the underestimation of simulated PFHpA and PFOA masses in the upper soil at the end of experiment might the reason, assuming a similar underestimation was also found before the vegetation period.

Parameter distribution

The optimized ranges and the initial ranges of substance parameters are given in Table 3 and Table 4 and in Additional file 1: Table S14–17. Although the initial parameter range was the same for all soil layers, the optimization found the substances more adsorptive to the upper soil layers (Additional file 1: Table S1), which are in fact more sorptive due to higher organic carbon content and mineral content (clay and silt). The upper boundaries of the parameter ranges were approached in several cases. An adjustment of the parameter ranges would have been a possibility, but was not done following the modeling strategy. Noticeable are the extreme differences of subsoil K_D-values for both diPAP. The high ranges of K_D values can be explained by a correlation to the degradation rate and the Freundlich n. The datapoint of diPAP masses in

the third soil layer, which is the transition layer between upper and lower soil, is the only datapoint available to calibrate diPAP parameters for lower soil, which results in a high uncertainty in the found parameter values. Compared with another modeling study [41], optimized values of K_D are higher for all PFAA in this study. The transport could be enhanced by different study conditions: in the present study, PFAA were slowly produced over time and in the comparing study, they were applied as a mixture on the soil surface, having more adsorption competition. A comparison of the optimized K_D values of PFAA and literature, where upper and lower soil was comparable to this study [18], show that the modeled range fits the magnitude of the measured values quite well, supporting the results of the optimization.

Results of Freundlich n values are shown in Additional file 1: Table S16. Values in the complete initial range (0.7–1.3) in case of PFPeA and 6:2 diPAP, values between 1 and 1.3 in case of PFHxA, values at the upper boundary in case of PFHpA and PFOA and values at the lower range (8:2 diPAP) were found. Reasons for a wide range could be a not given sensitivity or equifinality, since higher K_D and lower n might result in the same value of sorption strength, especially if the information content

Table 3 Initial parameter ranges and posterior parameter statistics of degradation rate $\mu_{ref,l,mi}$ and NER formation $\mu_{ref,s,mi}$ (1/days) of behavioral models

Substance	Min	5th	50th	95th	Max	Initial range
	$\mu_{ref,l,mi}$ at 20 °C					
	1/days					
6:2 diPAP	0.154	0.390	0.842	1.350	1.834	0–2
8:2 diPAP	0.312	0.351	0.488	0.657	0.722	0–2
Substance	$\mu_{ref,s,mi}$					
	10^{-3}/days					
PFOA	0.234	1.090	1.646	2.151	2.594	0–1000

Table 4 Initial parameter ranges and posterior parameter statistics of solute concentration factor (f_c) for plant uptake of behavioral models

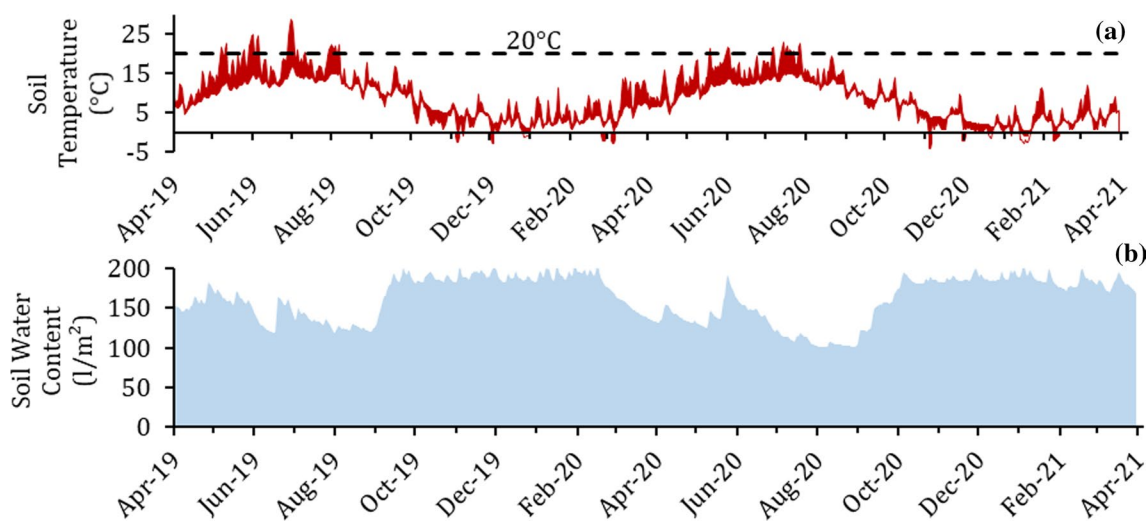| Precursor	Substance	Min	5th	50th	95th	Max	Initial range
		f_c (10^{-3})					
6:2 diPAP	PFPeA	0.00	54.7	93.8	117	117	0–1000
	PFHxA	4.11	5.47	7.30	11.1	14.8	0–1000
	6:2 diPAP	0.26	0.65	1.23	1.93	3.01	0–1000
8:2 diPAP	PFHpA	0.62	0.62	0.73	1.11	1.11	0–1000
	PFOA	0.55	0.63	0.73	1.11	1.11	0–1000
	8:2 diPAP	0.41	0.51	0.67	0.76	0.82	0–1000

Fig. 5 Simulated minimum and maximum soil temperatures (°C) in the upper 30 cm (**a**). Simulated soil water content of the whole lysimeter (L/m²) (**b**) of an example simulation

of the measured values is not enough to parameterize a non-linear isotherm or if the isotherm is in fact linear.

Anion exclusion posterior parameter statistics (Additional file 1: Table S17) show a complete use of the range for PFPeA and PFHxA and values at the boundary of initial values for PFHpA and PFOA. The small initial range of anion exclusion for the PFAA was the result of an internal model error when a bigger range was used as in [41]. An increase of the upper boundary of anion exclusion was rejected due to sufficient model results and only their maximum being on the boundary.

Results of degradation rate of diPAP $\mu_{ref,l,mi}$ and NER rate $\mu_{ref,s,mi}$, only regarding PFOA, are given in Table 3. NER rate of PFOA had a similar magnitude to the given optimized range of PFOA from other modeling studies: $1.5–4.4 \cdot 10^{-3}$/days [41], $3.0–6.6 \cdot 10^{-3}$ 1/days [38] with the range being overall lower, which might be the result of small differences in the soil composition.

Degradation rates of diPAPs are in a wide range, with the maximum value of 8:2 diPAP being lower than the maximum value of 6:2 diPAP and the minimum value being the opposite. This might be the result of interaction with other parameters, such as K_D-value compensating for changes in the value of the degradation rate, ending up in equifinality. The ranges of degradation rate of 6:2 diPAP are similar (0.45 1/days, strategy II) to another modeling study [41], but one order of magnitude higher than in a laboratory study [19], where transformation rates were calculated with a first-order degradation (0.048 1/days). Degradation rate of 8:2 diPAP is one order of magnitude higher compared with another modeling study (0.05 1/days,

strategy II) [41] and two orders of magnitudes higher than in a laboratory study [19], in which the rate had a value of 0.006 1/days. A possible reason for differences is the uncertainty of transformation dynamics between start and end of study, which was estimated through leaching dynamics of transformation products in this study and in another simulation study [41], and was measured in the laboratory study [19] with more data points for calculations. Furthermore, the rates calculated in this study were affected by soil moisture and temperature (Eq. 1). Thus, the actually used transformation rates during the modeling process were presumably lower most of the time, when optimum degradation conditions were not present. Additionally, in soils with saturated zones, the soil moisture factor in the degradation rate calculations of MACRO might not be suitable, because the degradation can decrease at high soil moisture due to low oxygen level [60], as discussed in [41].

The calibrated factor f_c is dependent on the chain length of PFAS (see Table 4), which can be attributed to the decreasing water solubility with increasing chain length [61]. Previously calibrated uptake factors for PFOA [38], showed values one to three orders of magnitude lower than the values obtained here. Other reasons for differences between the various uptake factors for PFOA are (1) different uptake factors for different plant species [62]; (2) different values for substance parameters, which also influence the uptake factor; and (3) a lower contamination situation here compared to Gassmann et al. 2021 [38], with uptake masses of > 0.1 mg per year.

Some of the substance parameters are correlated with each other, which means that other parameter combinations can also lead to similarly good results, since certain effects can be represented by different parameter values. A mutual influence was observed, for example, between the K_D value and the degradation rate ($r_{8:2 \text{ diPAP}} = 0.85$, $p < 0.001$), the K_D value and NER formation ($r_{\text{PFOA}} = -0.55$, $p < 0.01$), the K_D value and Freundlich n ($r_{\text{PFHpA}} = 0.56$, $p < 0.001$ und $r_{\text{PFHxA}} = 0.55$, $p < 0.001$), K_D value and f_c for 6:2 diPAP and the upper soil ($r_{8:2 \text{ diPAP}} = 0.85$, $p < 0.001$), Freundlich n value and fc for 6:2 diPAP ($r_{6:2 \text{ diPAP}} = -0.72$, $p < 0.001$) and K_D value and $\mu_{\text{ref,l,mi}}$ for both diPAP ($r_{6:2 \text{ diPAP}} = 0.91$, $p < 0.001$ and $r_{8:2 \text{ diPAP}} = 0.96$, $p < 0.001$) with high significance levels determined through the Pearson rank correlation test (Additional file 1: Table S18 and S19). The connection lies in the sorption equilibrium for the mentioned parameters. The lower the K_D value, the more is present in the liquid phase, and vice versa. To achieve a similar effect, a decrease in the K_D value should be accompanied by a reduction in the degradation rate in the liquid phase or an increase in NER formation in the solid phase. The significant correlations were not equally observed for all substances in the mentioned combinations.

Implications for contamination cases

When considering Fig. 5, the relationship between simulated temperatures and soil moisture content becomes evident, showing an inverse correlation (r = −0.73, $p < 0.001$), which can be attributed to evapotranspiration.

For the model, this modified approach suggests that high temperatures (spring/summer) and high moisture content, but still unsaturated (fall/winter), favor the degradation process. Therefore, degradation would occur throughout the year, except during temperatures below 0 °C, as degradation is not considered at these temperatures in the MACRO model if the temperature-dependent degradation is enabled. For real cases of diPAP contamination, a worst-case scenario for leaching of transformation products towards groundwater would occur during a mild summer with precipitation or precipitation after a warm but not dry period and in soils with a high water permeability, such as the sandy soils. This favors leaching of transformation products, such as at the beginning of fall until spring. Figure 5 also shows that the optimum conditions for transformation are hardly reached at all.

Another study [39], which simulated PFOA with and without precursor transformation in the saturated zone could be connected to a model such as presented here, to predict the leaching in the unsaturated soil for real contamination scenarios.

Conclusions

The use of models to represent the behavior of PFAS in the environment is crucial given the recorded cases of contamination. Results show that the transformation, leaching of diPAPs and their transformation products, soil retention, and plant uptake can be represented with the chosen model setup in MACRO. The influence of temperature and soil moisture on the transformation of diPAP worked to represent observed values, but the calculation of the transformation rate based on temperature and soil moisture was directly adopted from the model and should be investigated separately to verify this approach and potentially make adjustments if necessary.

Supplementary Information

Additional file 1: Table S1. Properties of soil interpolated for MACRO according to (Weidemann et al., 2022). **Table S2.** Acronyms, common names, chemical formulas, and molecular weights of in the text referenced PFAS. Information taken from Bell et al. (2019) and Zhao et al. (2013). **Table S3**. Means and standard deviations of percolate (L/m^2) and transformation products (µg) of the 6:2 diPAP lysimeters (n = 2). **Table S4.** Means and standard deviations of percolate (L/m^2) and transformation products (µg) of the 8:2 diPAP lysimeters (n = 2). **Table S5.** Means and standard deviations of transformation products (µg) in grass of the 6:2 diPAP lysimeters (n = 2). **Table S6.** Means and standard deviations of transformation products (µg) in grass of the 8:2 diPAP lysimeters (n = 2). **Table S7.** Means and standard deviations of transformation products (µg) and 6:2 diPAP in soil layers of the 6:2 diPAP lysimeters (n = 2). **Table S8**. Means and standard deviations of transformation products (µg) and 8:2 diPAP in soil layers of the 8:2 diPAP lysimeters (n = 2). **Table S9.** Relevant physical parameters and soil properties from the MACRO parameter input. Marked parameters are part of the water flow calibration. **Table S10.** Settings from the MACRO parameter input file. **Table S11.** Relevant crop parameter values from the MACRO parameter input file. **Table S12.** Relevant site parameter values from the MACRO parameter input file. **Table S13.** Diffusion coefficient in free water for different PFAS used in parameter input file. **Table S14.** Initial parameter range and posterior parameter statistics of saturated hydraulic conductivity, Van Genuchten's alpha and initial volumetric soil water content in behavioral models. **Table S15.** Initial parameter range, posterior parameter statistics and values found in Weidemann and Gassmann (2023) of sorption coefficient K_D (l/kg) of behavioral models. **Table S16.** Initial parameter ranges and posterior parameter statistics of Freundlich n (-) of soil of behavioral models. **Table S17.** Initial parameter ranges and posterior parameter statistics of anion exclusion θ_{AE} (%) of behavioral models. **Table S18.** Pearson rank correlation coefficient (r) and p-value of substance parameters of 6:2 diPAP simulation. **Table S19.** Pearson rank correlation coefficient (r) and p-value of substance parameters of 8:2 diPAP simulation. **Table S20.** P (Precipitation, L/m^2) and P* (precipitation after correction, L/m^2) according to Richter (1995). **Figure S1.** The mean relative distribution of 6:2 and 8:2 diPAP and their respective transformation products. **Figure S2.** Mean observed and modeled values and best compromise of percolate of 6:2 diPAP lysimeters (L/interval). **Figure S3.** Mean observed and modeled values and best compromise of percolate of 8:2 diPAP lysimeters (L/interval).

Availability of data and materials
The data used in the model are available in given tables in the publication or in the supporting information. The MACRO 5.2 model is available at https://www.slu.se/en/Collaborative-Centres-and-Projects/SLU-centre-for-pesticides-in-the-environment/models/macro-52/. Further information can be provided via contact of the corresponding author.

Declarations

Ethics approval and consent to participate
Not applicable.

Consent for publication
Not applicable.

Competing interests
The authors declare no conflicts of interest.

Author details
[1]Department of Hydrology and Substance Balance, University of Kassel, Kurt-Wolters-Straße 3, 34125 Kassel, Germany. [2]Department of Trace Analysis & Environmental Monitoring, Fraunhofer Institute for Molecular Biology and Applied Ecology IME, Auf dem Aberg 1, 57392 Schmallenberg, Germany. [3]School of Clinical Sciences at Monash Health, Faculty of Medicine, Nursing and Health Sciences, Monash University, Clayton, VIC 3800, Australia.

References
1. Voulgaropoulos A (2022) Mitigation of PFAS in US public water systems: future steps for ensuring safer drinking water. Env Prog and Sustain Energy. https://doi.org/10.1002/ep.13800
2. US Environmental Protection Agency (2021) PFAS|EPA: PFAS structures in DSSTox (update August 2021). https://comptox.epa.gov/dashboard/chemical-lists/PFASSTRUCTV4. Accessed 15 Jun 2022
3. Woodlief T, Vance S, Hu Q, DeWitt J (2021) Immunotoxicity of Per- and polyfluoroalkyl substances: insights into short-chain PFAS exposure. Toxics. https://doi.org/10.3390/toxics9050100
4. Pelch KE, Reade A, Wolffe TAM, Kwiatkowski CF (2019) PFAS health effects database: protocol for a systematic evidence map. Environ Int 130:104851. https://doi.org/10.1016/j.envint.2019.05.045
5. Buck RC, Franklin J, Berger U, Conder JM, Cousins IT, de Voogt P, Jensen AA, Kannan K, Mabury SA, van Leeuwen SPJ (2011) Perfluoroalkyl and polyfluoroalkyl substances in the environment: terminology, classification, and origins. Integr Environ Assess Manag 7:513–541. https://doi.org/10.1002/ieam.258
6. Houtz EF, Sutton R, Park J-S, Sedlak M (2016) Poly- and perfluoroalkyl substances in wastewater: significance of unknown precursors, manufacturing shifts, and likely AFFF impacts. Water Res 95:142–149. https://doi.org/10.1016/j.watres.2016.02.055
7. Weidemann E, Lämmer R, Stahl T, Göckener B, Bücking M, Breuer J, Kowalczyk J, Just H, Boeddinghaus RS, Gassmann M (2022) Leaching and transformation of PFAA and diPAP in unsaturated soil column studies. Environ Toxicol Chem. https://doi.org/10.1002/etc.5417
8. Trier X, Granby K, Christensen JH (2011) Polyfluorinated surfactants (PFS) in paper and board coatings for food packaging. Environ Sci Pollut Res 18:1108–1120. https://doi.org/10.1007/s11356-010-0439-3
9. Bugsel B, Bauer R, Herrmann F, Maier ME, Zwiener C (2022) LC-HRMS screening of per- and polyfluorinated alkyl substances (PFAS) in impregnated paper samples and contaminated soils. Anal Bioanal Chem 414:1217–1225. https://doi.org/10.1007/s00216-021-03463-9
10. Guo R, Liu X, Liu J, Liu Y, Qiao X, Ma M, Zheng B, Zhao X (2020) Occurrence, partition and environmental risk assessment of per- and polyfluoroalkyl substances in water and sediment from the Baiyangdian Lake. China Sci Rep 10:4691. https://doi.org/10.1038/s41598-020-61651-6
11. de Silva AO, Allard CN, Spencer C, Webster GM, Shoeib M (2012) Phosphorus-containing fluorinated organics: polyfluoroalkyl phosphoric acid diesters (diPAPs), perfluorophosphonates (PFPAs), and perfluorophosphinates (PFPIAs) in residential indoor dust. Environ Sci Technol 46:12575–12582. https://doi.org/10.1021/es303172p
12. Just H, Göckener B, Lämmer R, Wiedemann-Krantz L, Stahl T, Breuer J, Gassmann M, Weidemann E, Bücking M, Kowalczyk J (2022) Degradation and plant transfer rates of seven Fluorotelomer Precursors to Perfluoroalkyl acids and F-53B in a soil-plant system with maize (*Zea mays* L.). J Agric Food Chem. https://doi.org/10.1021/acs.jafc.1c06838
13. Rovero M, Cutt D, Griffiths R, Filipowicz U, Mishkin K, White B, Goodrow S, Wilkin RT (2021) Limitations of current approaches for predicting groundwater vulnerability from PFAS contamination in the vadose zone. Ground Water Monit Remediat 41:62–75. https://doi.org/10.1111/gwmr.12485
14. Röhler K, Susset B, Grathwohl P (2023) Production of perfluoroalkyl acids (PFAAs) from precursors in contaminated agricultural soils: batch and leaching experiments. Sci Total Environ 902:166555. https://doi.org/10.1016/j.scitotenv.2023.166555
15. Chen H, Reinhard M, Nguyen VT, Gin KY-H (2016) Reversible and irreversible sorption of perfluorinated compounds (PFCs) by sediments of an urban reservoir. Chemosphere 144:1747–1753. https://doi.org/10.1016/j.chemosphere.2015.10.055
16. Milinovic J, Lacorte S, Rigol A, Vidal M (2016) Sorption of perfluoroalkyl substances in sewage sludge. Environ Sci Pollut Res Int 23:8339–8348. https://doi.org/10.1007/s11356-015-6019-9
17. Schäffer A, Kästner M, Trapp S (2018) A unified approach for including non-extractable residues (NER) of chemicals and pesticides in the assessment of persistence. Environ Sci Eur 30:51. https://doi.org/10.1186/s12302-018-0181-x
18. McLachlan MS, Felizeter S, Klein M, Kotthoff M, de Voogt P (2019) Fate of a perfluoroalkyl acid mixture in an agricultural soil studied in lysimeters. Chemosphere 223:180–187. https://doi.org/10.1016/j.chemosphere.2019.02.012
19. Liu C, Liu J (2016) Aerobic biotransformation of polyfluoroalkyl phosphate esters (PAPs) in soil. Environ Pollut 12:230–237. https://doi.org/10.1016/j.envpol.2016.01.069
20. Fabregat-Palau J, Vidal M, Rigol A (2021) Modelling the sorption behaviour of perfluoroalkyl carboxylates and perfluoroalkane sulfonates in soils. Sci Total Environ 801:149343. https://doi.org/10.1016/j.scitotenv.2021.149343
21. Zhang Q, Wu X, Lyu X, Gao B, Wu J, Sun Y (2022) Effects of anionic hydrocarbon surfactant on the transport of perfluorooctanoic acid (PFOA) in natural soils. Environ Sci Pollut Res 29:24672–24681. https://doi.org/10.1007/s11356-021-17680-3
22. Liu J, Lee LS, Nies LF, Nakatsu CH, Turcot RF (2007) Biotransformation of 8:2 fluorotelomer alcohol in soil and by soil bacteria isolates. Environ Sci Technol 41:8024–8030. https://doi.org/10.1021/es0708722
23. Wang N, Szostek B, Buck RC, Folsom PW, Sulecki LM, Gannon JT (2009) 8–2 fluorotelomer alcohol aerobic soil biodegradation: pathways, metabolites, and metabolite yields. Chemosphere 75:1089–1096. https://doi.org/10.1016/j.chemosphere.2009.01.033

24. Lämmer R, Weidemann E, Göckener B, Stahl T, Breuer J, Kowalczyk J, Just H, Boeddinghaus RS, Gassmann M, Kling H-W, Bücking M (2022) Evaluation of the transformation and leaching behavior of two Polyfluoroalkyl phosphate diesters in a field lysimeter study. J Agric Food Chem. https://doi.org/10.1021/acs.jafc.2c03334

25. Cheng Y, Ding J, Xie X, Ji X, Zhang Y (2019) Validation and application of a 3-step sequential extraction method to investigate the fraction transformation of organic pollutants in aging soils: a case study of dechlorane plus. Environ Sci Technol 53:1325–1333. https://doi.org/10.1021/acs.est.8b06201

26. Zhou E, Crawford RL (1995) Effects of oxygen, nitrogen, and temperature on gasoline biodegradation in soil. Biodegradation 6:127–140. https://doi.org/10.1007/BF00695343

27. Leahy JG, Colwell RR (1990) Microbial degradation of hydrocarbons in the environment. Microbiol Rev 54:305–315. https://doi.org/10.1128/mr.54.3.305-315.1990

28. Cho Y-G, Rhee S-K, Lee S-T (2000) Effect of soil moisture on bioremediation of chlorophenol-contaminated soil. Biotech Lett 22:915–919. https://doi.org/10.1023/A:1005612232079

29. Tao L, Yang H (2011) Fluroxypyr biodegradation in soils by multiple factors. Environ Monit Assess 175:227–238. https://doi.org/10.1007/s10661-010-1508-2

30. Chaudhry Q, Blom-Zandstra M, Gupta S, Joner EJ (2005) Utilising the synergy between plants and rhizosphere microorganisms to enhance breakdown of organic pollutants in the environment. Environ Sci Pollut Res Int 12:34–48. https://doi.org/10.1065/espr2004.08.213

31. Anjos CS, Lima RN, Porto ALM (2021) An overview of neonicotinoids: biotransformation and biodegradation by microbiological processes. Environ Sci Pollut Res 28:37082–37109. https://doi.org/10.1007/s11356-021-13531-3

32. Vanclooster M, Boesten J, Trevisan M, Brown CD, Capri E, Eklo OM, Gottesbüren B, Gouy V, van der Linden A (2000) A European test of pesticide-leaching models: methodology and major recommendations. Agric Water Manag 44:1–19. https://doi.org/10.1016/S0378-3774(99)00081-5

33. Spill C, Gassmann M (2022) Long-term Sulfamethazine (SMZ) leaching simulation in two different soils using the MACRO model. J Environ Qual. https://doi.org/10.1002/jeq2.20337

34. García-Santiago X, Garrido JM, Lema JM, Franco-Uría A (2017) Fate of pharmaceuticals in soil after application of STPs products: influence of physicochemical properties and modelling approach. Chemosphere 182:406–415. https://doi.org/10.1016/j.chemosphere.2017.05.049

35. Jalali M, Farahani EA, Jalali M (2022) Simulating phosphorus leaching from two agricultural soils as affected by different rates of phosphorus application based on the geochemical model PHREEQC. Environ Monit Assess 194:164. https://doi.org/10.1007/s10661-022-09828-6

36. Raschke A, Nejadhashemi AP, Rafiei V (2022) Overview of modeling, applications, and knowledge gaps for integrated large-scale PFAS modeling. J Environ Eng. https://doi.org/10.1061/(ASCE)EE.1943-7870.0002033

37. Silva JAK, Šimůnek J, McCray JE (2020) A modified HYDRUS model for simulating PFAS transport in the vadose zone. Water 12:2758. https://doi.org/10.3390/w12102758

38. Gassmann M, Weidemann E, Stahl T (2021) Combined leaching and plant uptake simulations of PFOA and PFOS under field conditions. Environ Sci Pollut Res 28:2097–2107. https://doi.org/10.1007/s11356-020-10594-6

39. Gefell MJ, Huang H, Opdyke D, Gustafson K, Vlassopoulos D, McCray JE, Best S, Carey M (2022) Modeling PFAS fate and transport in groundwater, with and without precursor transformation. Ground Water 60:6–14. https://doi.org/10.1111/gwat.13152

40. Bierbaum T, Klaas N, Braun J, Nürenberg G, Lange FT, Haslauer C (2023) Immobilization of per- and polyfluoroalkyl substances (PFAS): comparison of leaching behavior by three different leaching tests. Sci Total Environ 876:162588. https://doi.org/10.1016/j.scitotenv.2023.162588

41. Weidemann E, Gassmann M (2023) transformation and leaching simulation of 6:2 and 8:2 diPAP and related metabolites in unsaturated soil column studies with MACRO. Environ Model Assess. https://doi.org/10.1007/s10666-023-09936-8

42. Persson J, Andersson N (2016) Modeling groundwater flow and PFOS transport: a case study at the old fire drill site of Bromma Stockholm Airport. https://urn.kb.se/resolve?urn=urn:nbn:se:kth:diva-189509. Accessed 20 Feb 2024

43. Goode DJ, Senior LA (2020) Groundwater Withdrawals and Regional Flow Paths at and near Willow Grove and Warminster, Pennsylvania -Data Compilation and Preliminary Simulations for Conditions in 1999, 2010, 2013, 2016, and 2017. https://doi.org/10.3133/ofr20191137

44. Gredelj A, Polesel F, Trapp S (2020) Model-based analysis of the uptake of perfluoroalkyl acids (PFAAs) from soil into plants. Chemosphere 244:125534. https://doi.org/10.1016/j.chemosphere.2019.125534

45. Shin H-M, Vieira VM, Ryan PB, Detwiler R, Sanders B, Steenland K, Bartell SM (2011) Environmental fate and transport modeling for perfluorooctanoic acid emitted from the Washington Works Facility in West Virginia. Environ Sci Technol 45:1435–1442. https://doi.org/10.1021/es102769t

46. Schaefer CE, Lavorgna GM, Lippincott DR, Nguyen D, Christie E, Shea S, O'Hare S, Lemes MCS, Higgins CP, Field J (2022) A field study to assess the role of air-water interfacial sorption on PFAS leaching in an AFFF source area. J Contam Hydrol 248:104001. https://doi.org/10.1016/j.jconhyd.2022.104001

47. Guo B, Zeng J, Brusseau ML (2020) A mathematical model for the release, transport, and retention of per- and polyfluoroalkyl substances (PFAS) in the vadose zone. Water Resour Res. https://doi.org/10.1029/2019wr026667

48. Larsbo M, Jarvis N (2003) MACRO 5.0. A model of water flow and solute transport in macroporous soil: Technical description. https://www.slu.se/globalassets/ew/org/centrb/ckb/modeller_dokument/macro-5.0-technical-report-2003.pdf. Accessed 20 Feb 2024

49. Larsbo M (2020) MACRO 5.2: MACRO a model of water flow and solute transport in macroporous soil. https://www.slu.se/en/Collaborative-Centres-and-Projects/SLU-centre-for-pesticides-in-the-environment/models/macro-52/. Accessed 20 Feb 2024

50. Stefan Reichenberger (2014) Technical note about potential (PET) and actual evapotranspiration (AET) and their components; implications for modelling with MACRO and PRZM. Footways S.A.S

51. Boesten JJTI, Linden AMA (1991) Modeling the influence of sorption and transformation on pesticide leaching and persistence. J Environ Qual 20:425–435. https://doi.org/10.2134/jeq1991.00472425002000020015x

52. Larsbo M Changes from earlier versions of MACRO 5. https://www.slu.se/en/Collaborative-Centres-and-Projects/SLU-centre-for-pesticides-in-the-environment/models/macro-52/. Accessed 20 Feb 2024

53. Schroll R, Becher HH, Dörfler U, Gayler S, Grundmann S, Hartmann HP, Ruoss J (2006) Quantifying the effect of soil moisture on the aerobic microbial mineralization of selected pesticides in different soils. Environ Sci Technol 40:3305–3312. https://doi.org/10.1021/es052205j

54. DWD Climate Data Center (2023) Tägliche Raster der potentiellen Evapotranspiration über Gras: Version 0.x. https://opendata.dwd.de/climate_environment/CDC/grids_germany/daily/evapo_p/

55. DWD Climate Data Center (2023) Datensatzbeschreibung: Tägliche Raster der potentiellen Evapotranspiration über Gras, Version 0.x. https://opendata.dwd.de/climate_environment/CDC/grids_germany/daily/evapo_p/BESCHREIBUNG_gridsgermany_daily_evapo_p_de.pdf

56. Lee H, D'eon J, Mabury SA (2010) Biodegradation of polyfluoroalkyl phosphates as a source of perfluorinated acids to the environment. Environ Sci Technol 44:3305–3310. https://doi.org/10.1021/es9028183

57. Gavrilescu M (2005) Fate of pesticides in the environment and its bioremediation. Eng Life Sci 5:497–526. https://doi.org/10.1002/elsc.200520098

58. Gupta HV, Kling H, Yilmaz KK, Martinez GF (2009) Decomposition of the mean squared error and NSE performance criteria: implications for improving hydrological modelling. J Hydrol 377:80–91. https://doi.org/10.1016/j.jhydrol.2009.08.003

59. Monteil C, Zaoui F, Le Moine N, Hendrickx F (2020) Multi-objective calibration by combination of stochastic and gradient-like parameter generation rules–the caRamel algorithm. Hydrol Earth Syst Sci 24:3189–3209. https://doi.org/10.5194/hess-24-3189-2020

60. Kästner M, Nowak KM, Miltner A, Trapp S, Schäffer A (2014) Classification and modelling of nonextractable residue (NER) formation of xenobiotics in soil–a synthesis. Crit Rev Environ Sci Technol 44:2107–2171. https://doi.org/10.1080/10643389.2013.828270

61. Bell CH, Gentile M, Kalve E, Ross I, Horst J, Suthersan S (2019) Emerging contaminants handbook. CRC Press, Boca Raton

62. Lasee S, Subbiah S, Thompson WA, Karnjanapiboonwong A, Jordan J, Payton P, Anderson TA (2019) Plant uptake of PFAAs under a maximum

bioavailability scenario. Environ Toxicol Chem. https://doi.org/10.1002/etc.4571

Publisher's Note

Springer Nature remains neutral with regard to jurisdictional claims in published maps and institutional affiliations.